

## **A LONG LIFETIME BALLOON-BORNE CRYOSTAT AND MAGNETIC REFRIGERATOR**

J. O. Gundersen<sup>1,3</sup>, M. Jirmanus<sup>2</sup>, P. Timbie<sup>1</sup>, Z. Zhao<sup>2</sup>,  
S. Cordone<sup>1</sup>, and Y. Lin<sup>2</sup>.

<sup>1</sup>Department of Physics, University of Wisconsin  
Madison, WI, 53706, USA

<sup>2</sup>Janis Research Company, Inc.  
Wilmington, MA 01887, USA

<sup>3</sup>Current Address: Department of Physics, Princeton University  
Princeton, NJ 08544

### **ABSTRACT**

A long lifetime, low cost, vapor-shielded liquid neon and liquid helium cryostat and an adiabatic demagnetization refrigerator have been developed for cooling a bolometric radiometer to 0.1 K for mm and sub-mm observations of the cosmic microwave background. This is the first phase of a development effort for a very long hold time system for use in NASA's 100 Day Ultra Long Duration Balloon Project. This type of system has additional applications in sub-orbital and ground-based research in millimeter, sub-millimeter, infrared, and x-ray astrophysics. A detailed description of the design, analysis, and performance of the system is presented and plans for follow-up design improvements are discussed.

### **INTRODUCTION**

A prototype long lifetime cryostat and two-stage adiabatic demagnetization refrigerator (ADR) have been constructed to support the National Aeronautics and Space Administration's (NASA) Ultra-Long Duration Balloon (ULDB) Project.<sup>1</sup> The primary design goals for this prototype instrument were a 10 day lifetime for the liquid helium (LHe) and liquid neon (LNe) cryogens and a 48 hour lifetime between recycling at 0.1 K for the two-stage ADR. This instrument is suitable for cooling far-infrared bolometers<sup>2</sup> for sub-orbital and ground-based research in millimeter, sub-millimeter, and infrared astrophysics, as well as laboratory testing of x-ray microcalorimeters for sub-orbital research in x-ray

astrophysics.<sup>3,4</sup> Many of the design features from this prototype can be implemented in an instrument that supports the 100 day lifetime requirements of NASA's ULDB Project. In addition to astrophysics, there are several commercial applications that this type of cryogenic system can support. These applications include the cooling of x-ray microcalorimeters used in microanalysis<sup>5</sup> for the semiconductor industry and for cooling superconducting tunnel junctions<sup>6,7</sup> and transition edge sensors used in heavy particle detection<sup>8</sup> for studying biological samples and DNA sequencing. The project objectives are summarized, the cryostat and two-stage ADR design and performance are reviewed, and future plans for this type of system are discussed.

## PROJECT OBJECTIVES

The principal objective was to design and construct a lightweight, low cost, long lifetime LHe-LNe cryostat and a two-stage ADR capable of cooling bolometric detectors to 0.1 K. Since this project was funded by the first phase of a NASA Small Business Innovative Research<sup>9</sup> (SBIR) grant, the design, fabrication, and testing of this cryogenic system had to be completed in six months. In the process of modeling and building this prototype we have gained the experience that is necessary to construct a 100 day hold time LHe-LNe ADR system for NASA's ULDB program. The technical objectives are divided into those that relate to the LHe-LNe cryostat, those that relate to the two-stage ADR, and those that relate to the integration and testing of the combined ADR and the LHe-LNe cryostat.

As with spacecraft instrumentation, one of the primary constraints on balloon-borne instrumentation is weight. The maximum weight of the science instrumentation for a 10 day, long duration balloon<sup>10</sup> (LDB) flight around Antarctica is 1360 kg, while the science payload limit for the demonstration 100 day ULDB payload is 910 kg.<sup>1</sup> For this project, a target weight of 140 kg was set and achieved for the filled cryostat and two-stage ADR. The remaining science weight is typically used for the gondola superstructure, the optical system, the electronics, and the power, guidance, and telemetry systems. For comparison, this cryostat is a factor of three lighter than the LHe/liquid nitrogen (LN) cooled <sup>3</sup>He cryostat flown in the BOOMERANG LDB project.<sup>11</sup> Unlike spacecraft instrumentation, balloon-borne projects are funded at considerably lower levels – typically an order of magnitude below a Small Explorer class satellite. Hence the relative cost of a balloon-borne cryostat compared to a space-borne system has to reflect this funding difference. This cryogenic system was constructed with the aid of a SBIR Phase I grant of \$70,000 and an additional \$17,000 of supplemental internal funding. This cryostat is designed to support a LDB flight, which typically has a duration of 10 days. The cryostat incorporates a rugged design to withstand the parachute shock that occurs at the termination of a balloon flight and causes as much as 10 g vertical deceleration and 5 g at 45° from the vertical.<sup>12</sup>

For the above applications, the ADR is required to cool detectors below 0.1 K. Single-stage ADRs can reach these temperatures when operated from a bath temperature of ~2 K. The two-stage ADR is a natural extension of the single stage ADR that was developed<sup>13</sup> for NASA's Space Infrared Telescope Facility (SIRTF) and is based on the concept forwarded by Haggmann and Richards.<sup>2</sup> The detailed design for the two-stage ADR was obtained from J. Martinis and collaborators<sup>5</sup> at the National Institute of Standards and Technology (NIST). In order to fulfil the project goals within the stringent time constraints of a Phase I SBIR grant, we chose to replicate the NIST design with minor modifications. The primary motivation for building a two-stage ADR (versus a single stage ADR) is that it can operate either from an unpumped, 4 K LHe bath or a 4 K cryocooler. A LHe bath was

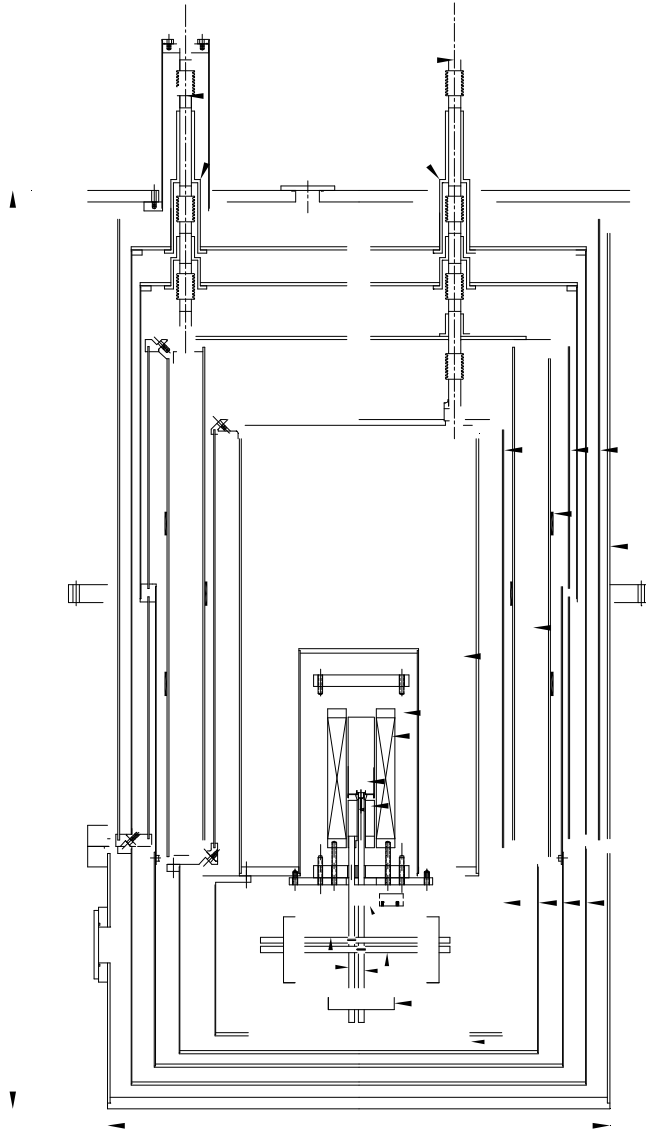


**Figure 1.** Schematic of LNe/LHe cryostat and two-stage ADR.

used rather than a 4 K cryocooler because of the vibration and power consumption constraints of balloon-borne, bolometric observations. The capability of operating from a 4 K bath simplifies the ground based operations immensely and alleviates the need for a superfluid bath at balloon altitudes. Balloon-borne LHe cryostats typically allow the atmosphere to pump on the LHe bath as the payload ascends to 40 km where the ambient pressure is 4-5 Torr. Roughly half the LHe is lost during this process. In a balloon flight that uses a two-stage ADR, the pressure above the LHe bath could be regulated to one atmosphere, doubling the LHe hold time.

The cryostat and two-stage ADR were integrated for testing at the University of Wisconsin, Madison (UWM). The primary objectives of the testing procedure were to measure the temperatures of the vapor cooled shields, measure the evaporation rates of the cryogens to establish hold times, and verify the operation of the two-stage ADR. All but the last of these objectives were met within the time constraint of the SBIR. Due to vendor-related delays associated with the delivery of the cryostat support tubes, the testing of the two-stage ADR didn't occur until several weeks after the SBIR deadline. The results from these tests are discussed in more detail below.

## LIQUID HELIUM-LIQUID NEON CRYOSTAT

### Cryostat Design

The cryostat design, shown in Figure 1, incorporates two superinsulated, vapor-cooled shields, a LHe reservoir and a LNe reservoir. The interwoven design of radiation shields and support tubes was inspired by the design of a rocket-borne ADR system.<sup>3,4</sup> This modular design allows full access to all reservoirs and radiation shields and includes a 22 L LNe reservoir and a 19.5 L LHe reservoir. The escaping cryogen vapors pass through heat exchangers<sup>14</sup> at each warmer stage on the fill/vent lines. The LHe reservoir has a re-entrant space to accommodate the two-stage ADR. The LNe volume is toroidal in shape and is used as the secondary cryogen for three reasons:

1. LNe was chosen over LN because its lower temperature significantly reduces the conductive and radiative loads on the LHe.
2. LNe was chosen over liquid hydrogen for safety reasons.
3. LNe was chosen over a pure LHe cryostat because a liter of LNe can absorb approximately seven times more heat than a liter of LHe used to vapor cool a shield at 27 K, assuming 100% vapor cooling efficiency (VCE).<sup>15</sup> VCE is defined as the ratio of the enthalpy used to the total enthalpy available at each heat exchanger.

The additional cost of using LNe (~\$120/L) versus LN (~\$1/L) for a balloon flight is trivial compared to the overall costs of ballooning. For preflight and laboratory use, the LNe is easily replaced with LN and a several day hold time is obtained.

The primary compromise in the design of the cryostat occurred when the 1.6 mm thick G-10 tubes were delivered late and out of specification by an outside vendor. In order to finish the project on a six month schedule, a decision was made to replace the G-10 with 0.74 mm thick stainless tubes. This reduced the ultimate hold time significantly, but the 10 day target hold time was still met by minor adjustments in the design and the LNe and LHe reservoir capacities. This modification was accompanied by a detailed finite element analysis<sup>16</sup> (FEA) thermal model of the cryostat in three different configurations:

1. Stainless steel tubing and a 300 K vacuum shell
2. G-10 tubing and a 300 K vacuum shell
3. G-10 tubing and a 240 K vacuum shell

The third configuration simulates balloon-borne temperatures and assumes one atmosphere pressure regulation of the liquid cryogens. Results of this analysis and the cryostat performance are given in the next section.

### Cryostat Performance

The first extended cold test of the cryostat used LHe and LN (instead of LNe) and did not include the ADR and its associated wiring. This test resulted in a static evaporation rate of 250 mL/hr of LHe, 19 mL/hr of LN and temperatures of 210 K and 150 K for the outer and inner vapor cooled shields (OVCS/IVCS). A FEA model was constructed using these experimental results. The model predicts the final VCS temperatures and the heat load into the two reservoirs as a function of the VCE at the neon reservoir and the two VCS. The result of this analysis indicated that the data is best fit with a VCE of 50% at the neon reservoir, 32% at the IVCS and 43% at the OVCS. The refined FEA performed after the first test was subsequently used to predict the performance of the cryostat under various conditions. The results are shown in Table 1. Due to time constraints, no further testing and effort was expended to improve the heat exchange between the escaping gas and the various stages.

**Table 1.** Predicted cryostat performance.

Case Number	Support Tube	Vacuum Shell (K)	OVCS (K)	IVCS (K)	LHe/LNe Evaporation Rate (mL/hour)	LHe/LNe Hold Time (Days)
1*	S/S	300	205	121	50/93	16/10
2	G-10	300	253	150	20/30	41/31
3	G-10	240	195	115	20/15.5	41/59

\*Measured performance for Case 1 was within 5% of predicted performance.

After installing the ADR, the heat switch, and the associated temperature sensors into the cryostat, additional measurements with LHe and LNe were performed to establish the system performance. Both the temperatures and evaporation rates agreed within 5% of the FEA model for Case 1. The FEA model also calculates the total radiative and conductive loads on each of the cryogenic stages. The chart in Figure 2 shows these results for the Case 1 configuration of the cryostat. The FEA model was then used to predict two other configurations given above. The estimated temperatures, evaporation rates, and hold times for each of these configurations are given in Table 1.

This cryostat met the goal of a 10 day hold time with the LNe being the limiting cryogen. If this cryostat were instrumented for a LDB flight using infrared bolometers, a vacuum window would be required along with openings down to the LHe level. This, combined with extra loading from instrumentation wiring, would make this cryostat unusable for a LDB flight in its current configuration. However, if this cryostat were refitted with G-10 supports, then it would be more than adequate for a LDB flight. Furthermore, based on the Case 3 analysis, a scaled up version of this cryostat, with more sophisticated heat exchangers, would be well suited for a ULDB flight. In the last section, additional improvements are discussed which could reduce the reservoir sizes.

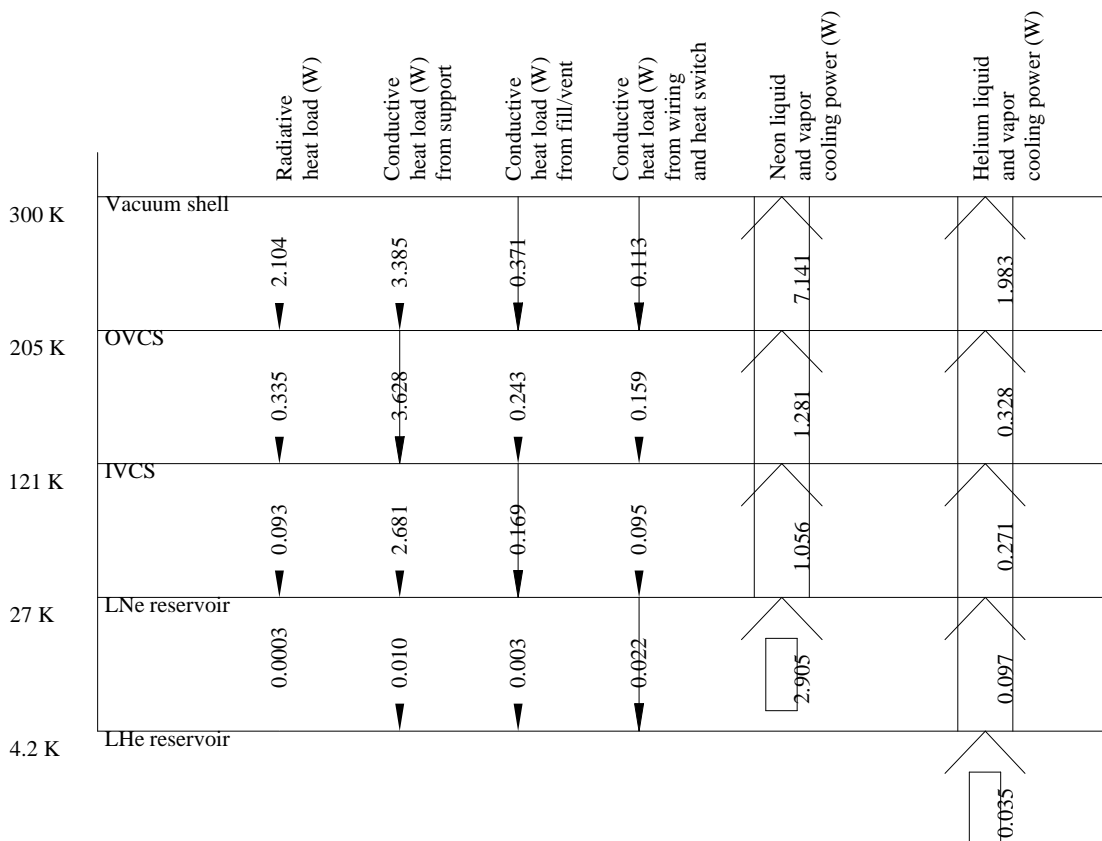


**Figure 2.** Heat map for the LHe/LNe cryostat with stainless support tubes (Case 1) with 50 and 100 mL/hour evaporation rates for LHe and LNe, respectively.

## TWO-STAGE ADIABATIC DEMAGNETIZATION REFRIGERATOR

### ADR Design

The two-stage ADR was fabricated based on a design developed at NIST<sup>5</sup> and is shown inside the cryostat in Figure 1. A brief review of the design is given here, while the interested reader should contact J. Martinis<sup>17</sup> for specific details. The two-stage ADR consists of two paramagnetic pills, a Kevlar<sup>®18</sup>-69 suspension system, a magnet, a magnet shield, and a heat switch. The two paramagnetic pills are composed of a ferric ammonium alum (FAA) salt and a gadolinium-gallium garnet (GGG) crystal. The FAA pill was grown at the UWM and is based on the SIRTf design.<sup>13</sup> Annealed gold wires of 99.999% purity permeate the FAA and couple heat from a gold-plated copper rod that is attached to the suspension system. The GGG pill was purchased commercially<sup>19</sup> and is similarly coupled to a gold-plated copper rod that is attached to the suspension system. During operation the GGG pill reaches a temperature of ~1 K and intercepts the heat load from the 4 K stage. The pills reside within the bore of a 4 T, superconducting magnet.<sup>20</sup> The magnet and pills are surrounded by a 1.51 cm thick magnet shield of heat treated Hiperco<sup>21</sup> (a Fe-Co-V alloy generally known as vanadium permendur) which reduces the field outside the shield to less than 1 mT<sup>13</sup> (10 gauss). Commercially available high  $T_c$  superconducting leads<sup>22</sup> are used between the LNe and LHe stage to minimize the Joule heating of the LHe during the magnetization process and to minimize conductive loading. A manually actuated heat switch<sup>23</sup> simultaneously couples the FAA and GGG pills to the 4 K bath during magnetization. A segmented tube (not shown in Figure 1) is coupled to a rotary feedthrough at 300 K and a right angle gear box at 4 K, and the tube is rotated to actuate the heat switch. The segmented tube is composed of thin wall stainless sections that run between the radiation shields and small copper sections that are used at the rotary feedthroughs of each radiation shield to assist in heat sinking.

### ADR Performance

The ADR was tested in a series of measurements at UWM. Since the primary objective in these first tests was to confirm device operation, a very simple experimental set up was used: A stable power supply was used to directly set the magnet current, while the salt pill temperatures were monitored using germanium resistance thermometers. Other than the Kevlar<sup>®</sup> suspension system, the only connection to the cold stages was the thermometry wiring. The wiring to the 0.1 K stage was buffered by heat sinking on the 1 K stage.

A general discussion of magnetic refrigeration may be found in many references.<sup>24</sup> The operation of this ADR involves the following steps:

1. The magnet is ramped up to full current (~8.5 A) with the heat switch closed so that the heat of magnetization generated in the pills is rejected to the 4K bath.
2. The heat switch is opened, thermally isolating the pills from the bath, and the magnet is demagnetized.

Roughly, since the entropy  $S=S(B,T)$  and the system is adiabatically isolated ( $\Delta S=0$ ), controlling the magnetic field  $B$  applied to the pills controls the salt pill temperatures. In practice, this provides a convenient means for temperature regulation in the sub-Kelvin temperature range. The magnet current can be reduced until the desired operating temperature is reached, and then an electrical feedback circuit may be used to further reduce the magnet current to compensate for parasitic loading, such that the cold stage is thermostatically regulated. During the initial ADR test, the magnet was ramped to zero field and a minimum temperature of 0.06 K was obtained. For our 83 g FAA pill this can be

translated to an ability to sink 91 mJ while regulating at 0.1 K. The magnetic field was then increased until the FAA stabilized at a temperature of 0.1 K. The warm up rate at this temperature was measured to be 650  $\mu$ K/hour, which corresponds to a parasitic load of 160 nW. Given this amount of loading, we estimate the hold time we would achieve regulating at 0.1 K to be six days. This represents an upper limit, since other demands on the cooling capacity, such as additional wiring for detector signals, would reduce the hold time. This estimate is also complicated by the fact that the GGG pill does not remain at constant temperature when the FAA pill temperature is regulated, since they share the bore of the same magnet. The GGG reached 0.9 K with 55 mT applied field (the field at which the FAA pill reached 0.1 K), and warmed 2.2 mK/hour at this temperature. The actual temperature drifts in the GGG that would be induced due to changes in the field regulating the 0.1 K stage and the resulting changes in conductive loading on the FAA are difficult to estimate. Nevertheless, it is clear that even a pessimistic estimate of the hold time, when compared to the cycling time of ~45 minutes, yields a 0.1 K duty cycle of better than 99%.

## FUTURE DIRECTIONS

There are several modifications that would improve this cryogenic system's performance in either ground-based or balloon-borne operations.

- 1) The stainless support system needs to be replaced with a G-10 support system. Janis has recently manufactured a similar cryostat with this type of G-10 support system.<sup>25</sup> This will significantly decrease the conductive heat loads at all stages in the cryostat.
- 2) A remotely operable heat switch is required for balloon-borne operations, and this would also make ground based operations more convenient. One solution is to place a computer controlled stepper motor on the externally actuated heat switch.
- 3) The high  $T_c$  leads are the largest contributors to the 4 K conductive loading assigned to the wiring and heat switch in Figure 2. The length of these leads can easily be doubled reducing this conductive heat load by almost a factor of two.
- 4) A magnet controller is required to stabilize the ADR temperature for bolometric measurements. This is currently being built based on an existing rocket-borne ADR system.<sup>3,4</sup>

A list of other improvements that would be suitable for a future ULDB cryogenic system is given here.

- 1) A more efficient heat exchanger system would be required for an ULDB cryostat. This has been realized in a cryogenic system that has recently been built by Janis.<sup>25</sup>
- 2) A system to solidify the LNe would further reduce the conductive loads on the LHe. A solid Ne reservoir has worked well in a cryogenic system for the ASTRO-E satellite.<sup>26</sup>
- 3) A more compact ADR suspension system would allow for a larger instrument volume and reduce the area of the radiation shields yielding a reduction in the radiative loads on all stages.

Finally, we are investigating a low vibration, low power consumption 4 K cryocooler that could be coupled to the two-stage ADR. This would require a complete cryostat redesign; however, if the cryocooler induced microphonics can be minimized, a cryocooled two-stage ADR is an ideal solution for an ULDB cryogenic system.

## ACKNOWLEDGEMENTS

The authors wish to acknowledge Dan McCammon, Scott Porter and Peter Shirron for helpful discussions regarding cryostat design, John Martinis for enabling the fabrication of the two-stage ADR, and Karen Lewis and Chris O'Dell for assistance in salt pill fabrication. This work was performed at Janis Research Company and the University of Wisconsin-Madison and was supported by NASA Phase I SBIR contract # NAS5-98119.

## REFERENCES

1. <http://www.wff.nasa.gov/~uldb/>.
2. C. Hagmann and P.L. Richards, Two-stage magnetic refrigerator for astronomical applications with reservoir temperatures above 4 K, *Cryogenics*, 34:221(1994).
3. W. Cui, R. Almy, S. Deiker, D. McCammon, J. Morgenthaler, W.T. Sanders, R.L. Kelley, F. J. Marshall, S.H. Moseley, C.K. Stahle, and A.E. Szymkowiak, A sounding rocket experiment employing microcalorimeter detectors to obtain a high-resolution spectrum of the diffuse X-ray background, *SPIE Proc.* 2280:362 (1994).
4. D. McCammon, R. Almy, S. Deiker, J. Morgenthaler, R.L. Kelley, F.J. Marshall, S.H. Moseley, C.K. Stahle, and A.E. Szymkowiak, A sounding rocket payload employing high-resolution microcalorimeters, *Nucl. Instr. Meth. Phys. Res. A* 370:266 (1996).
5. D.A. Wollman, K.D. Irwin, G.C. Hilton, L.L. Dulcie, D.E. Newbury, and J.M. Martinis, High-resolution energy-dispersive microcalorimeter spectrometer for X-ray microanalysis, *J. Of Microscopy*, 188, Part 3, p. 196 (1997).
6. C.A. Mears, S.E. Labov, M. Frank, M.A. Lindeman, L.J. Hiller, H. Netel, and A.T. Barfknecht, Analysis of pulse shape from a high resolution superconducting tunnel junction and x-ray spectrometer, *Nucl. Instr. Meth. Phys. Res. A* 370:53 (1996).
7. T. Twerenbold, J.L. Vuilleumier, D. Gerber, A. Tadsen, B.v.d. Brandt, and P.M. Gillevet, Detection of single macromolecules using a cryogenic particle detector coupled to a biopolymer mass spectrometer. *Appl. Phys. Lett.* 68 (24), 3503 (1996).
8. G.C. Hilton, J.M. Martinis, D. Twerenbold, P.M. Gillevet, D.A. Wollman, K.D. Irwin, L.L. Dulcie, and D. Gerber, Impact energy measurement in time-of-flight mass spectrometry with cryogenic microcalorimeters, *Nature*, 391:672 (1998).
9. <http://sbir.nasa.gov/>.
10. <http://master.nsf.nasa.gov/>.
11. <http://astro.caltech.edu/~jgg/boom/>.
12. National Scientific Balloon Facility Handbook, Palestine, TX.
13. P.T. Timbie, G.M. Bernstein, and P.L. Richards, Development of an adiabatic demagnetization refrigerator for SIRTf, *Cryogenics*, 30:271 (1990).
14. D. Steffensrud, J. Bahls, E. Christenson, K. Fassnacht, E. Guckel, D. Harriman, S. Nahn, P. Vu, and J. Xiang, Efficiency of short heat exchangers for helium vapor cooling, *Rev. Sci. Instr.* 62, 1, 214 (1991).
15. J.E. Jensen, W.A. Tuttle, R.B. Stewart, H. Brechna, and A. Prodell, Eds. "Brookhaven National Laboratory Selected Cryogenic Data Notebook," National Technical Information Service, Springfield, VA (1980), II-F-1, V-E-1.
16. ANSYS, Inc., Cannonsburg, PA, release 5.3, thermal and structural finite element analysis software.
17. J. Martinis, National Institute of Standards and Technology, Boulder, CO 80303.
18. Kevlar® is a registered DuPont trademark.
19. Litton Industries, Inc., Airtron Div., SYNOPTICS, Charlottesville, NC.
20. American Magnetics, Inc., Oak Ridge, TN.
21. Arnold Engineering Co., Marengo, IL.
22. BICC Cables Limited, Wrexham, England.
23. Infrared Laboratories, Tuscon, AZ.
24. Pobell, F., "Matter and Methods at Low Temperature," Springer (1996), p. 169.
25. A. Nash, P. Shields, M. Jirmanus, and Z. Zhao, Development of the FACET cryostat, preprint submitted for publication in *Adv Cryog Eng* (1999).
26. S.M. Volz, K. Mitsuda, H. Inoue, Y. Ogawara, M. Hirabayashi, and M. Kyoya, The X-ray Spectrometer (XRS): a multi-stage cryogenic instrument of the Astro-E x-ray astrophysics mission, *Cryogenics*, 36:763 (1996).